Eur. Phys. J. C 49, 163–167 (2007)
DOI 10.1140/epjc/s10052-006-0106-5

THE EUROPEAN PHYSICAL JOURNAL C

Regular Article – Experimental Physics

Study of the ALICE performance for the measurement of beauty via the electron decay channel

M. Lunardon[1,2,a] for the ALICE Collaboration

[1] University of Padova, 35122 Padova, Italy
[2] INFN Sezione di Padova, Via Marzolo 8, 35131 Padova, Italy

Received: 3 August 2006 /
Published online: 16 November 2006 –

Abstract. We present a strategy for the detection of electrons coming from the semi-electronic decay of beauty particles generated in Pb–Pb and p–p collisions at LHC using the ALICE detector. The experiment's performance for this measurement is evaluated in terms of accessible p_t range and expected uncertainties.

PACS. 25.75.-q, 12.38.Mh, 13.20.He

1 Introduction

In a few years the large hadron collider (LHC), presently under construction at CERN, will deliver lead beams at an energy as high as 2.75 TeV/nucleon. In a central lead–lead collision a huge energy will be released in a small volume (of the order of $10^3\,\text{fm}^3$), thus recreating conditions present in the early universe only a few microseconds after the Big Bang. Under such extreme conditions the formation of a deconfined state of quarks and gluons is expected.

In the study of the properties of this deconfined system, heavy quarks play a crucial role for several reasons:

– due to their large virtuality, the production time scale is of the order of $0.1\,\text{fm}/c$ or less, well shorter than the expected lifetime of the deconfined state ($\approx 10\,\text{fm}/c$). Thus they can experience the full collision history and provide information on the medium properties.
– Hard partons are expected to lose energy while propagating through the medium. The recent experimental observations in Au–Au collisions at RHIC [1–4] have generated an intense theoretical activity aimed at understanding the origin and the dependencies of such observables. In the models (see for example [5]) the energy loss is predicted to depend both on the colour-charge and on the mass of the traversing parton. A comparative study of the attenuation of massless, charm and beauty probes at the LHC will provide essential information to test the interpretation of the energy loss effects and to further investigate the properties of the medium itself.
– The production cross section at the LHC energies is predicted to be large [6], allowing for high statistics measurements.

Moreover the measurement of the beauty cross section is important for the study of quarkonia production, one of the historic quark gluon plasma observables [7], as it will provide a) the natural normalization for the analysis of bottomonium production at the LHC and b) the amount of $B \to J/\psi$ contamination to the J/ψ yield.

2 Heavy flavour detection in ALICE

ALICE [6] is the experiment in preparation at the LHC specifically designed for tracking and identification of the particles produced in heavy-ion collisions. The capability of ALICE for the detection of heavy-flavour particles relies, in particular, on the following:

– *tracking and vertexing*: the inner tracking system (ITS), the time projection chamber (TPC) and the transition radiation detector (TRD), embedded in a magnetic field $B \leq 0.5\,\text{T}$, allow track reconstruction in the pseudo-rapidity range $|\eta| < 0.9$ with a transverse momentum (p_t) resolution better than 2% for $p_t < 10\,\text{GeV}/c$ and a track transverse impact parameter (d_0[1]) resolution better than $60\,\mu$m for $p_t > 1\,\text{GeV}/c$, mainly provided by the two innermost layers of the ITS (forming the silicon pixel detector – SPD);
– *particle identification*: good particle identification (PID) in a wide p_t range is achieved in ALICE by combining the capabilities of various detectors: charged hadrons are identified using time-of-flight (TOF) and specific energy loss $\mathrm{d}E/\mathrm{d}x$ (ITS, TPC) measurements.

[a] marcello.lunardon@pd.infn.it

[1] The transverse impact parameter d_0 is defined here as the minimum distance between the track and the primary vertex projected on the plane perpendicular to the beam direction

Electrons with momentum higher than $1\,\mathrm{GeV}/c$ are separated from pions in the TRD, using the transition radiation techinque, and in the TPC, by the $\mathrm{d}E/\mathrm{d}x$ information. Muons are identified in the muon arm covering the backward pseudo-rapidity region $-4 < \eta < -2.5$.

The performance study discussed here is based on a detailed simulation of the detectors that we expect to provide a realistic description of the main experimental effects. The results shown hereafter refer mainly to Pb–Pb collisions at $\sqrt{s_{NN}} = 5.5$ TeV. The same analysis has been done for *p*–*p* collisions at $\sqrt{s_{NN}} = 14$ TeV and some of the final results are shown here. More details on the heavy flavour detection performance in the *p*–*p* system can be found in [8].

3 Simulation details

The production of open beauty can be studied by detecting the electrons originated in the semi-electronic decays of beauty hadrons. Based on a recent NLO [9] calculation [10] we assumed for this study a beauty production yield of 4.6 $b\bar{b}$ pairs per central (0%–5% of the total cross section) Pb–Pb collision at $\sqrt{s_{NN}} = 5.5$ TeV, and a yield of 0.007 $b\bar{b}$ pairs per minimum bias *p*–*p* collision at $\sqrt{s_{NN}} = 14$ TeV. The corresponding calculations for charm predict a production yield for the two systems of 115 and 0.16 $c\bar{c}$ pairs respectively. It has to be noted that these predictions are affected by large uncertainties (a factor 2 to 3) depending on the choice of the quark masses and QCD scales.

Taking into account the semi-electronic branching ratio (about 10% each for both $b \to eX$ and $b \to c \to eX$ processes) and the ALICE acceptance (about 24%) we get a yield of beauty-originated electron (signal) per event of about 0.4 in Pb–Pb and 7×10^{-4} in *p*–*p*. These yields have to be extracted from the copious background of electrons from other sources, such as (a) charm-originated electrons, (b) photon conversions in the detector material, (c) Dalitz decays of light mesons (mainly pions), strange particle decays, and (d) hadrons misidentified as electrons. The number of electrons from source (a), based on the above calculations, is more than 20 times larger than the signal electrons and the contribution from sources (b),(c) and (d) is even larger. All the above sources have been considered in this study.

The simulation has been performed within the AliRoot [11] framework. In order to optimize the computing resources, we chose to treat separately the generation of signal and background. To produce the beauty sample we used PYTHIA6 with parameters tuned to reproduce the *c*- and *b*-quark p_t distributions from the NLO calculations [10], with the CTEQ4L parton distribution function set, modified for nuclear shadowing in Pb–Pb collisions using the EKS98 [12] parameterization. A semi-electronic decay with the electron in the detector acceptance has been required at the generation stage. A similar generation has been adopted for the charm electrons (background source (a)). For the background sources (b), (c) and (d) we used HIJING [13] for Pb–Pb collisions, which provides a density of charged particles per unit of rapidity $\mathrm{d}N_\mathrm{ch}/\mathrm{d}y = 6000$, and PYTHIA6 minimum bias for *p*–*p* collisions.

4 Selection of electrons from beauty hadrons

An effective selection of the beauty-originated electrons can be achieved in ALICE by exploiting the capability of resolving the secondary vertices generated by beauty hadrons decaying weakly in the semi-electronic channel. Due to the large mean life-time of beauty hadrons ($c\tau \approx 500\,\mu$m) the measured transverse impact parameter of signal electrons is larger on average than that of background electrons and can be used for the signal selection.

The second fundamental aspect is the electron identification: because of the huge number of pions produced in a nucleus-nucleus interaction at LHC energies, a very good pion rejection is needed. A first electron selection is made by the TRD. Detailed simulations and first test beam results [14,15] show that, for an electron efficiency $\epsilon(e) \approx 90\%$, a pion contamination $\epsilon(\pi) \approx 1\%$ is expected for electron momenta $p > 1\,\mathrm{GeV}/c$. The electrons can be further separated from pions looking at their specific energy loss ($\mathrm{d}E/\mathrm{d}x$) in the TPC [16,17]. Heavier hadrons are completely rejected by using the information of the TRD and TOF detectors. The final pion efficiency as a function of the momentum, for a fixed electron efficiency $\epsilon(e) \approx 80\%$, is shown in Fig. 1: at low momenta the fraction of pions misidentified as electrons is expected to be lower than 10^{-4}.

The effect of the particle identification and impact parameter cuts is summarized in Fig. 2, where we show the impact parameter distributions of electrons from different sources ($p_\mathrm{t} > 1\,\mathrm{GeV}/c$ has been selected). Before particle identification the spectrum is dominated by pions (upper dashed line). Electron identification brings the pion contribution to a negligible level, while electrons from charm (dot dashed) and other background sources (dotted) still represent most of the electrons. Then, by selecting a proper impact parameter lower threshold (200 μm in this case) we can make beauty (solid) to be the main contribution on the selected electron sample.

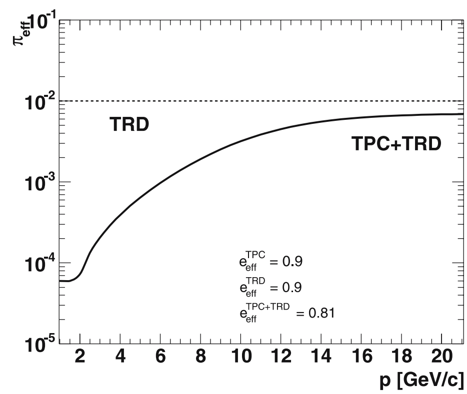

Fig. 1. Fraction of pions misidentified as electrons after combined PID in TRD + TPC as a function of pion momentum

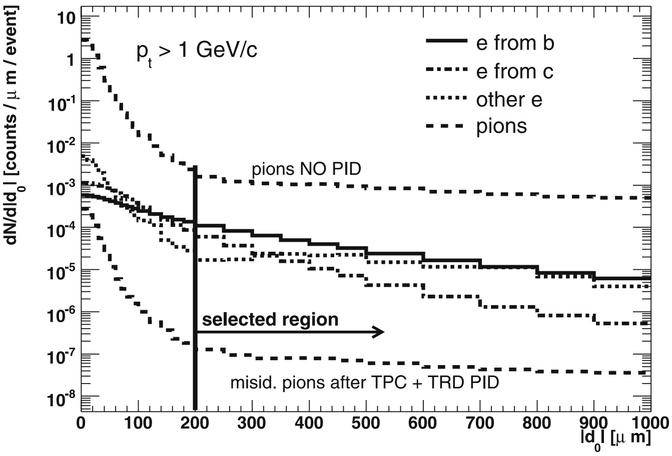

Fig. 2. Impact parameter distributions of electrons coming from different sources. After PID and proper d_0 cut electrons from beauty dominate the selected electron sample. See text for details

The optimal value for the impact parameter cut is determined as a function of p_t by minimizing the expected uncertainty. The residual contamination from charm and other background sources can be evaluated and subtracted. The details are discussed on the next section.

5 Evaluation of the expected sensitivity

The selection cuts have been optimized as a function of p_t by evaluating the expected sensitivity in term of statistical and systematic uncertainties. The reference statistics is 10^7 central (0%–5% of the total cross section) events, for the Pb–Pb sample, and 10^9 minimum bias events, for the p–p sample. This statistics is expected to correspond to about one year of data taking at the LHC at nominal luminosity [6].

The p_t-differential cross section of electrons from beauty can be extracted with the following procedure:

- in a given bin of p_t we count N candidate electrons. This number is the sum of N_b electrons from beauty, N_c electrons from charm and N_{bkg} background electrons or misidentified pions;
- the N_c contribution can be estimated using a Monte Carlo simulation tuned in the charm cross section extracted from the measurement of the the D^0 mesons in the $D^0 \to K^- \pi^+$ decay channel [18, 19];
- the N_{bkg} contribution can be similarly evaluated using the measured distributions of light hadrons;
- the number of beauty electrons $N_b = N - N_c - N_{bkg}$ is then corrected for detector efficiencies (tracking, PID and d_0 cut) and acceptance: $N_b^{corr} = N_b/\epsilon$;
- finally the obtained yield is normalized to one nucleon-nucleon collision (correction for the centrality class and the nucleon-nucleon inelastic cross section at $\sqrt{s_{NN}} =$ 5.5 TeV for Pb–Pb collisions or just the proton–proton inelastic cross section for p–p at 14 TeV).

The statistical and systematic uncertainties are computed as follow:
statistical uncertainty: for a given p_t bin, the relative statistical uncertainty is given by

$$\frac{\sigma(N_b^{stat})}{N_b} = \frac{\sqrt{N}}{N_b}\,, \qquad (1)$$

where N and N_b are the electron numbers defined above;
systematic uncertainties: various sources of systematic errors are expected:

- subtraction of charm contribution (N_c): the uncertainties in the measurement of the $D^0 \to K^- \pi^+$ (statistical and systematic) are propagated at the level of the p_t distribution of the electrons coming from charm semi-electronic decays. We assume that the cross sections of all charmed hadrons will be derived from the measured D^0 cross section. We estimated the relative systematic uncertainty introduced by this assumption to be about 4%. See [17] for more details;
- subtraction of other background contributions (N_{bkg}): in this study we assume that the p_t distributions of background electrons and misidentified pions will be affected by a 10% relative uncertainty over the whole p_t range;
- the relative uncertainty on the cross section normalization in Pb–Pb (p–p) is estimated to be 9% (5%) [18].

The p_t-dependent part of the total uncertainty (statistical + systematic) has been evaluated as a function of the d_0 threshold. As an example, we show in Fig. 3 the behaviour of the relative statistical (triangles) and p_t-dependent systematic (stars) uncertainties for electrons with $2.0 < p_t < 2.5$ GeV/c: as the d_0 threshold increases, the statistical part increases too (maximum statistics with no d_0 cut), while the systematic part decreases, since less and less background is left in the electron sample. The line

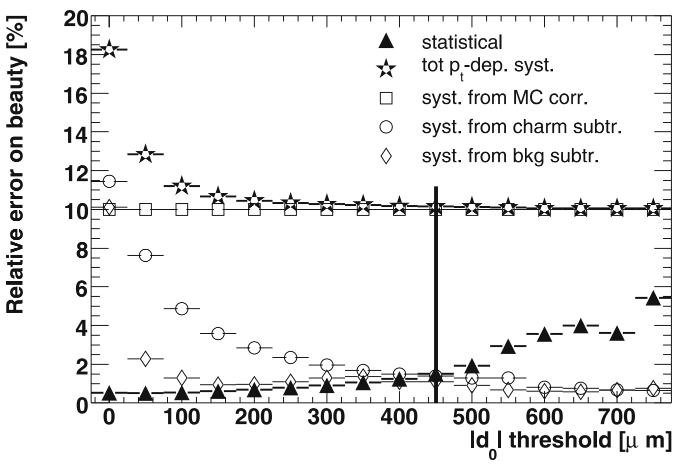

Fig. 3. Relative statistical (triangles) and total p_t-dependent systematic (*stars*) uncertainties for electrons with $2.0 < p_t <$ 2.5 GeV/c as a function of the d_0 threshold. Also shown the contributions to the total p_t-dependent systematic uncertainty: charm subtraction (*open circles*), other background subtraction (*open diamonds*) and MC corrections (*open squares*)

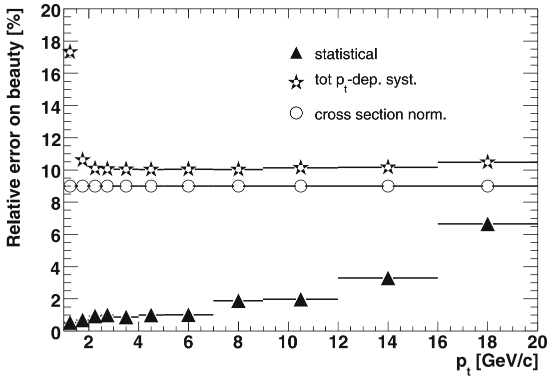

Fig. 4. Relative statistical (triangles) and total p_t-dependent systematic (*stars*) uncertainties as a function of p_t for the Pb–Pb system. The cross section normalization uncertainty is also shown (*open circles*)

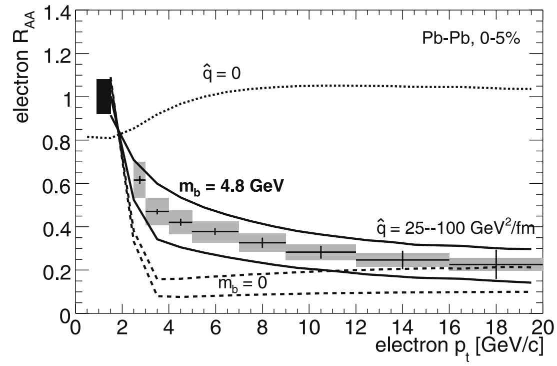

Fig. 6. Nuclear modification factor R_{AA} of electrons from beauty after one year of data taking at nominal luminosity. Statistical (*crosses*), p_t-dependent systematic (*filled gray area*) and normalization (*black area*) uncertainties are shown together with theoretical calculations for different energy loss scenarios. See text for details

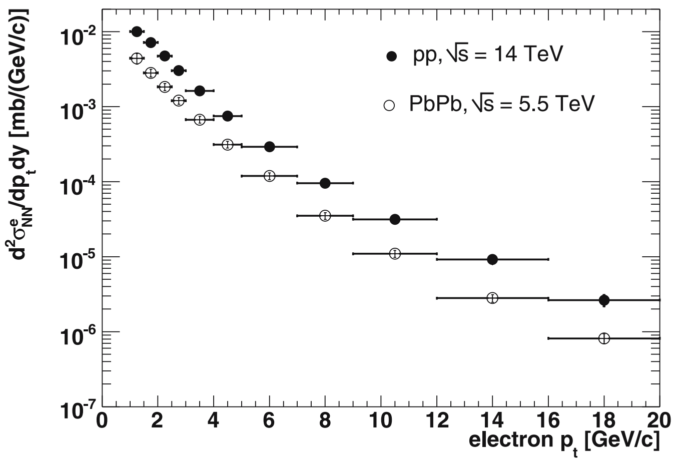

Fig. 5. Reconstructed p_t-differential cross sections of electrons from beauty per nucleon–nucleon collision in 10^7 central Pb–Pb events (*open circles*) and 10^9 minimum bias *p–p* events (*filled circles*). Statistical and p_t-dependent systematic uncertainties are shown

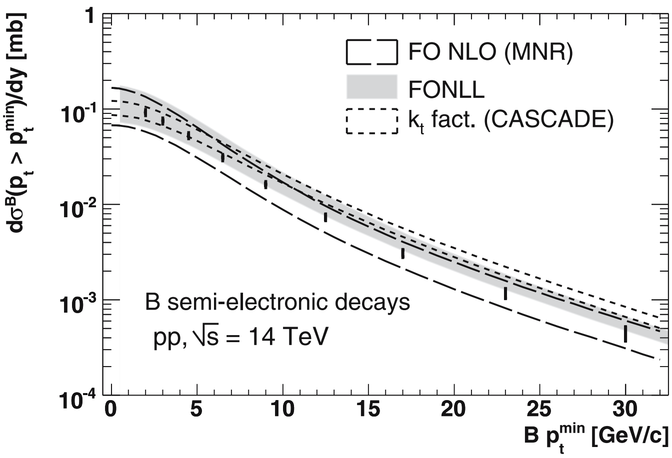

Fig. 7. Reconstructed p_t^{min}-differential cross section of B mesons in *p–p* @ $\sqrt{s_{NN}} = 14\,\text{TeV}$ as measured with 10^9 minimum-bias events. Statistical uncertainty (*inner bars*) and quadratic sum of statistical and p_t-dependent systematic uncertainty (*outer bars*) are shown; the normalization error is not shown. The theoretical predictions from three pQCD calculations with their uncertainty bands are also shown (see text)

at $|d_0| = 450\,\mu$m shows the impact parameter cut that minimizes the total uncertainty.

Using this procedure we defined an optimum d_0 threshold for each considered p_t bin, from $p_t = 1\,\text{GeV}/c$ to $p_t = 20\,\text{GeV}/c$. The estimated uncertainties as a function of p_t, in the case of the Pb–Pb system, are summarized in Fig. 4. In Fig. 5 we report the p_t-differential cross section per nucleon-nucleon collision of electrons coming from beauty with the uncertainties estimated with the above described procedure. The cross sections in Pb–Pb (open circles) and *p–p* (filled circles) systems are shown together.

The measured yields in *p–p* and Pb–Pb can be used to compute the nuclar modification factor R_{AA}: the ratio of the p_t distribution of electrons measured in Pb–Pb to the one measured in *p–p*, scaled by the average number of binary collisions N_{coll} in the selected centrality class (0–5% in this case). This observable is expected to be 1 if the nucleus–nucleus collision behaves as a simple superposition of N_{coll} independent nucleon-nucleon collisions. The suppression of this ratio at high p_t observed at RHIC [2–4] is a strong indication of in-medium phenomena such as the parton energy loss. Figure 6 shows the R_{AA} of electrons from beauty measured after one year of data taking at nominal luminosity. Theoretical calculations for different energy loss scenarios, depending on the in-medium transport coefficient $\hat{q}$ and on the b quark mass [20], are also shown. The band corresponding to $m_b = 4.8\,\text{GeV}$ and $\hat{q} = 25\text{–}100\,\text{GeV}^2/\text{fm}$ reflects the uncertainty of the model employed in this study. It can be seen that the predicted sensitivity of ALICE allows a meaningful comparison with the theory.

We also show in Fig. 7 how this expected sensitivity can be compared with the current theoretical predictions in the reconstructed p_t^{min}-differential cross section of B

mesons ($\mathrm{d}\sigma^B(p_\mathrm{t} > p_\mathrm{t}^\mathrm{min})/\mathrm{d}y$ vs. $p_\mathrm{t}^\mathrm{min}$ averaged over the range $|y| < 1$) for the p–p system, as extracted from the single electron cross section using a well known Monte Carlo procedure [21, 22]. In the same figure we report the results of three recent calculations with their theoretical uncertainty bands: a collinearly-factorized fixed order next-to-leading order (FO NLO) approach, as implemented in the HVQMNR code [9], the fixed order next-to-leading log (FO NLL) [23, 24] and the k_t-factorization approach, as implemented in the CASCADE code [25]. It can be seen that the expected ALICE performance for 10^9 p–p events will provide a meaningful comparison with pQCD predictions.

6 Conclusions

In the present study we investigated the performance of ALICE for the measurement of the beauty production at the LHC via the electron decay channel. The good capabilities of ALICE for the measurement of displaced tracks and electron identification should allow to select a clean sample of beauty-originated electrons and to reconstruct their p_t-differential cross section with good sensitivity from 1 up to 20 GeV/c.

References

1. STAR Collaboration, J. Adams et al., Phys. Rev. Lett. **91**, 072 304 (2003)
2. PHENIX Collaboration, S.S. Adler et al., Phys. Rev. Lett. **91**, 072 301 (2003)
3. PHOBOS Collaboration, B.B. Back et al., Phys. Lett. B **578**, 297 (2004)
4. BRAHMS Collaboration, I. Arsene et al., Phys. Rev. Lett. **91**, 072 305 (2003)
5. R. Baier, Y.L. Dokshitzer, A.H. Mueller, S. Peigné, D. Schiff, Nucl. Phys. B **483**, 291 (1997)
6. ALICE Collaboration, J. Phys. G **30**, 1517 (2004)
7. T. Matsui, H. Satz, Phys. Lett. B **178**, 416 (1986)
8. F. Antinori, C. Bombonati, M. Lunardon, A. Dainese, ALICE Internal Note, to be published as ALICE-INT-2006
9. M.L. Mangano, P. Nason, G. Ridolfi, Nucl. Phys. B **373**, 295 (1992)
10. N. Carrer, A. Dainese, ALICE Internal Note, ALICE-INT-2003-019 (2003)
11. ALICE Collaboration, http://aliceinfo.cern.ch/Offline
12. K.J. Eskola et al., hep-ph/0104010
13. M. Gyulassy, X.N. Wang, Phys. Rev. D **44**, 3501 (1991) http://www-nsdth.lbl.gov/∼xnwang/hijing
14. ALICE Technical Design Report of the Transition Radiation Detector, CERN/LHCC 2001-021
15. ALICE Collaboration, T. Mahmoud, et al., Nucl. Instrum. Methods A **502**, 127 (2003)
16. ALICE Technical Design Report of the Time Projection Chamber, CERN/LHCC 2000-001
17. F. Antinori, A. Dainese, M. Lunardon, R. Turrisi, ALICE Internal Note ALICE-INT-2005-033 (2006)
18. A. Dainese, Ph.D. Thesis, Università degli Studi di Padova (2003), arXiv:nucl-ex/0311004
19. N. Carrer, A. Dainese, R. Turrisi, J. Phys. G **29**, 575 (2003)
20. N. Armesto, A. Dainese, C.A. Salgado, U.A. Wiedemann, Phys. Rev. D **71**, 054 027 (2005)
21. UA1 Collaboration, C. Albajar et al., Phys. Lett. B **213**, 405 (1988)
22. UA1 Collaboration, C. Albajar et al., Phys. Lett. B **256**, 121 (1991)
23. M. Cacciari, M. Greco, P. Nason, JHEP **9805**, 007 (1998)
24. M. Cacciari, S. Frixione, P. Nason, JHEP **0103**, 006 (2001)
25. H. Jung, Comput. Phys. Commun. **143**, 100 (2002)